A Photogrammetric Simulator for Close-Range Applications

Tian-Yuan Shih

Abstract

Simulation is an important process for project design. An algorithm specifically designed for close-range applications is described in this study. This algorithm, based on human behavior, simulates the hand-held camera situation. The algorithm and a numerical example are presented. An implementation into a CAD system has been attempted, in which the initial results are rather encouraging.

Introduction

Through several years of application, photogrammetry has been verified to be an efficient and economically feasible method for spatial data gathering. Aerial photogrammetry functions as the major data acquisition tool for geographic information systems; meanwhile, close-range photogrammetry is becoming increasingly important for CAD/CAM applications. Reviewing the latest International Archives of Photogrametry and Remote Sensing (ISPRS, 1994), a number of close-range photogrammetry applications, related to CAD/CAM, have been reported. These applications include the refurbishment and upgrading of a petro-chemical plant (Chandler and Still, 1994), the reverse engineering for the flight deck of a commuter airliner (Stirling *et al.*, 1994), as well as architectural tasks (Streilein and Gaschen, 1994).

Simulation is an indispensable tool for modern surveying projects. Objectives such as network optimization, accuracy prediction, and other design goals all require simulation. Simulation also provides the optimum tool in studying those uncertain factors in a controllable manner, because "it provides more flexibility and unlimited variation in its parameters" (El-Hakim, 1984). Image data simulators, such as DATAGEN (Doyle, 1966; Woolnough, 1973; Owolabi, 1989) have been implemented since the early stage of photogrammetric development. An aerotriangulation package frequently consists of a simulation module, such as BLUH (Jacobsen, 1980), PSP (Tseng, 1992), and others.

Simulation for close-range applications has also been utilized extensively. The implementation is generally similar to those procedures used for aerial photography. The six exterior orientation parameters X_C, Y_C, Z_C, and ω, ϕ, κ are explicitly defined. Next, the image coordinates are generated with the given object space information and sensor specifications. Although a standard procedure, it is sometimes impractical, particularly for close-range applications with convergent photographs.

An algorithm is therefore designed in this study, which emulates the hand-held camera situation. For small objects, the photographer normally aims at the center of the object

Department of Civil Engineering, National Chiao-Tung University, 1001 Ta-Hsueh Road, Hsinchu, Taiwan, R.O.C.
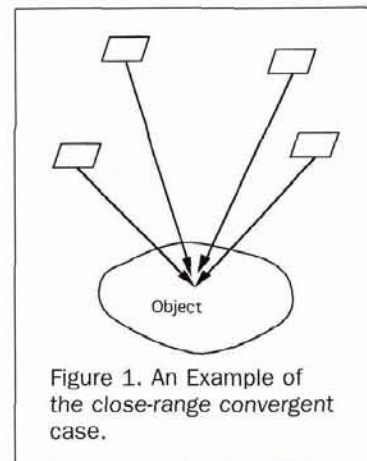

Figure 1. An Example of the close-range convergent case.

and either positions the camera horizontally or maintains it vertically (Figure 1). Analytically, this implies that either the x- or y-axis of the image coordinate system is parallel to the ground, frequently, the X-Y plane.

The Parameters for a Photogrammetric Simulator

Examining the mechanism of a photogrammetric simulator for aerial triangulation reveals that there are several parameters related to the flights, i.e.,

- The percentage of overlap and sidelap;
- The flying height;
- The number of strips and the number of photos in each strip;
- Ground point distribution, and/or the tie point distribution. These points are generally distributed in a grid pattern. The parameter, density of these points, is determined at the will of user;
- The variation range of exterior orientation parameters; and
- The standard deviation of the generated observations, namely, the ground coordinates, photo coordinates, and/or other observation such as the GPS deduced projective center related coordinates.

In addition, camera specifications, such as the focal length and the distortions, form another group of parameters. Instead of specifying the number of flight strips and photos in each strip, the other approach involves specifying the (north,

east) and (south, west) corners of the block. The ground control point file can often be edited by the user to satisfy practical requirements.

Due to the regularity of the aerial photo block, neither the coordinates of the projective centers nor the rotation elements of the sensor have to be explicitly specified by the user. Frequently, this is not the situation in close-range applications, where large tilt angles and convergent photography are commonly used. The other difference between an aerial and a close-range simulator is the image format. While the nine-inch (230-mm by 230-mm) format is the standard for aerial photography, several standards for close-range application are available. The formats frequently used include, 24mm by 36mm (135-mm Camera), 60mm by 60mm, and 230mm by 230mm (such as the Rollei LFC (A.R. Hoffman, personal communication, 1990) and the GSI CRC-1 (Brown, 1984)). Together with the use of digital still cameras and video cameras, the image format varies even more significantly, e.g., the active area of the Kodak Megapixel is 8.98 mm by 7.04 mm.

Based on the afore-mentioned considerations, four groups of parameters are included in the user interface of the presented close-range photogrammetric simulator, i.e.,

- The sensor specification: focal length, lens distortion, and image format;
- The object space information: editable by the user;
- The exterior orientation elements: positional and rotational; and
- The accuracy index: standard deviations for the simulated observations.

The Algorithm

Taking a photograph involves aiming at a focal point of the object, e.g., the center of the scene, with a tendency to maintain the camera either vertically or horizontally. This behavior results in the presented algorithm. As shown in Figure 2, when the projective center is fixed and the center of interest is selected, the direction of optical axis of the camera is defined. That is, the z-axis of the image coordinate system is fixed in the object coordinate system. The rotation of the image space x-y plane in the object space is fixed when the x-axis is constrained to be parallel to the object X-Y plane.

Mathematically, with the direction cosines of the given optical axis (l, m, n) and the horizontal constraint, the rotation matrix of the image coordinate system can be expressed as follows:

$$
R = \begin{pmatrix}
\dfrac{m}{\sqrt{l^2+m^2}} & \dfrac{-l}{\sqrt{l^2+m^2}} & 0 \\
\dfrac{ln}{\sqrt{l^2+m^2}} & \dfrac{mn}{\sqrt{l^2+m^2}} & \dfrac{-(l^2+m^2)}{\sqrt{l^2+m^2}} \\
l & m & n
\end{pmatrix} \tag{1}
$$

In this case, the rotation elements are computed with the algorithm and do not require being provided by the user. In a practical implementation, when the photo scale is given and the overlap percentage is specified, both the projective center and the center of interest can be generated with this algorithm, provided that sufficient information regarding the object is made available.

Two solutions to the rotation matrix are observed from the derivation stated in Appendix A. In the resulting rotation matrix, all the elements in both formulations have the same magnitude. The sign relations are illustrated in Figure 3.

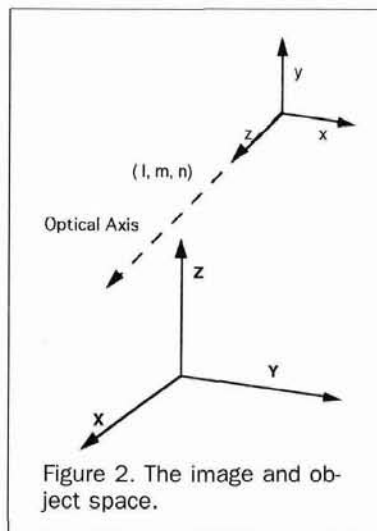Examining the following collinearity equations:

Figure 2. The image and object space.

$$
\begin{cases}
x = c\,\dfrac{m_{11}(X - X_C) + m_{12}(Y - Y_C) + m_{13}(Z - Z_C)}{m_{31}(X - X_C) + m_{32}(Y - Y_C) + m_{33}(Z - Z_C)} \\[2ex]
y = c\,\dfrac{m_{21}(X - X_C) + m_{22}(Y - Y_C) + m_{23}(Z - Z_C)}{m_{31}(X - X_C) + m_{32}(Y - Y_C) + m_{33}(Z - Z_C)}
\end{cases} \tag{2}
$$

The sign change of the first two rows of the rotation matrix indicates the sign change of the image coordinates.

For some applications, the convergence angle (Slama, 1980) is an important index. With the direction cosines of two optical axes (l_1, m_1, n_1) and (l_2, m_2, n_2), the sum of the convergence angle can be easily computed with Equation 3: i.e.,

$$
\cos \gamma = \frac{l_1 l_2 + m_1 m_2 + n_1 n_2}{\sqrt{l_1^2 + m_1^2 + n_1^2}\ \sqrt{l_2^2 + m_2^2 + n_2^2}} \tag{3}
$$

An Example

Two photographs are simulated for the given object space point distribution shown in Figure 4. The parameters chosen are

- focal length : 28 mm;
- point center on: $(X, Y, Z) = (11.0, 10., 11.5)$;
- the projective center
  photo 1: $(X_{C_1}, Y_{C_1}, Z_{C_1}) = (10.9, 7.0, 11.0)$;
  photo 2: $(X_{C_2}, Y_{C_2}, Z_{C_2}) = (11.2, 10.0, 11.5)$.

The Computed rotation matrices:

$$
\text{photo 1:} \begin{pmatrix}
0.999445 & -0.033315 & 0.000000 \\
0.005474 & 0.164219 & -0.986409 \\
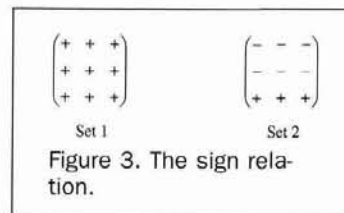0.032862 & 0.095861 & 0.164310
\end{pmatrix}
$$

Figure 3. The sign relation.

Front View   Side View
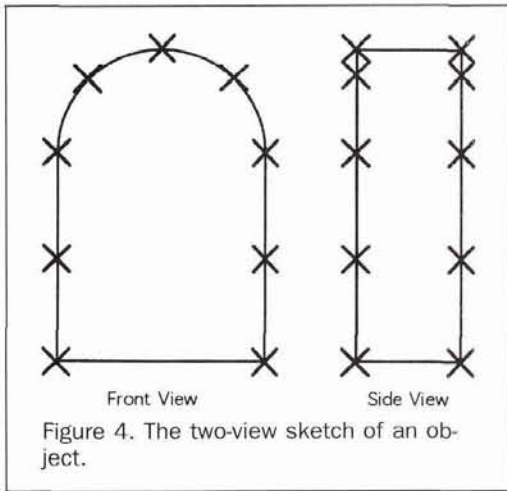
Figure 4. The two-view sketch of an object.

$$\text{photo 2:} \begin{pmatrix} 0.997785 & 0.066516 & 0.000000 \\ -0.010912 & 0.163681 & -0.986453 \\ -0.065618 & 0.984268 & 0.164045 \end{pmatrix}$$

The sum of the convergence angle is 5°38'43". The object coordinates and the generated image coordinates are listed in Table 1. Once the image coordinates have been generated, the next step involves verifying whether the image points lie inside of the image format or not. A window smaller than the actual image format, such as 22 mm by 34 mm for 24 mm by 36 mm, is normally used. Next, the random errors of specified distribution and magnitude can be generated and added on, with schemes such as those provided in Press *et al.* (1986) and Swan (1994).

Concluding Remarks

A photogrammetric simulator has been designed in this study for close-range applications. The function of this simulator is similar to the reaction of the operator, thereby being particularly suitable for a hand-held camera case. The project designed employing this algorithm can be easily executed because the instructions are clear and close to a human's normal reaction. The philosophy of the presented scheme describes the characteristics of human vision as well. That is, when one looks at an object, the optical axes of both eyes are centered on the object.

The computation load of the presented algorithm is relatively less than that of the version explicitly giving the exterior orientation parameters, because the rotation matrix is directly formed without any requirement for trigonometric terms.

An implementation of this algorithm in a CAD environment has been conducted as a result of the increasing linkage between CAD/CAM and close-range photogrammetry. The existing CAD model provides sufficient knowledge regarding the object for the simulation. Utilizing the visualization tools provided in the CAD software allows for a detailed examination of the simulated photo, not only from a metric point of view but also from a semantic one. It should be noted that, parallel to this study, a similar function has been implemented in a commercial photogrammetric system (Pomaska, 1994). This also provides additional support to the potential usefulness of the presented algorithm.

Acknowledgment

References

Brown, D.C., 1984. A Large Format, Microprocessor Controlled Film Camera Optimized for Industrial Photogrammetry, Presented paper, XV Congress of the International Society for Photogrammetry, Rio de Janeiro, June.

Chandler, J.H., and A.L. Still, 1994. Analytical Photogrammetry and the Refurbishment of the GAT Reformer , BP Refinery, Grangemouth, Scotland — Lessons Learnt, *International Archives of Photogrammetry and Remote Sensing*, 30(5):28-34.

Doyle, F.J., 1966. Fictitious Data Generator for Analytical Aerotriangulation, *Photogrammetria*, 21:179-194.

El-Hakim, S.F., 1984. *On the Detection of Gross and Systematic Errors in Combined Adjustment of Terrestrial and Photogrammetric Data*, Photogrammetric Research, Division of Physics, National Research Council of Canada, P-PR-54.

ISPRS, 1994. Close Range Techniques and Machine Vision, *International Archives of Photogrammetry and Remote Sensing*, 30(5), Proceedings of the Commission V Symposium, 1-4 March 1994, Melbourne, Australia.

Jacobsen, K., 1980. *Vorschläge zur Konzeption und zur Bearbeitung von Buendelblockausgleichungen*, Wissenschaftliche Arbeiten der Fachrichtung Vermessungswesen der Universität Hannover, Nr. 102.

Owolabi, K., 1989. *Simultaneous Distributional and Model Robustness in Photogrammetric Bundle Block Adjustment*, PhD Thesis, University of New Brunswick, Canada.

Pomaska, G., 1994. Simulation for Close Range Photogrammetric Applications in a CAD Environment, *International Archives of Photogrammetry and Remote Sensing*, 30(5):318-324.

Press, W.H., B.P. Flannery, S.A. Teukolsky, and W.T. Vetterling, 1986. *Numerical Recipes*, Chapter 7, Cambridge University Press, Cambridge.

Slama, C.C (editor), 1980. *Manual of Photogrammetry*, 4th Edition, American Society of Photogrammetry, Falls Church, Virginia.

Stirling, D.M., A.M. Bridger, and M.R. Shortis, 1994. Photogrammetric Modeling of a Commuter Airliner Flightdeck for Reverse Engineering Purposes, *International Archives of Photogrammetry and Remote Sensing*, 30(5):374-381.

Streilein, A., and S. Gaschen, 1994. Comparison of a S-VHS Camcorder and a High-Resolution CCD-Camera for Use in Architectural Photogrammetry, *International Archives of Photogrammetry and Remote Sensing*, 30(5):382-389.

Swan T., 1994. The Chip-is-Bad Fever, Dr. Dobb's Journal, 1994(1):111-113.

Tseng, Y.H., 1992. Tips for the Photogrammetric Software Package (PSP), draft obtained from the author.

TABLE 1. THE OBJECT AND IMAGE COORDINATES

Point	X	Y	Z	x_{p_1}	y_{p_1}	x_{p_2}	y_{p_2}
1	10	10	10	−10.13	14.94	−9.74	14.56
2	10	10	11	9.56	4.66	−9.22	4.66
3	10	10	12	−9.05	−4.52	−8.74	−4.23
4	10.292	10	12.707	−6.16	−10.39	−6.01	−10.06
5	11	10	13	0.00	−12.59	0.00	−12.58
6	11.707	10	12.707	6.06	−10.18	6.17	−10.49
7	12	10	12	8.86	−4.32	9.12	−4.61
8	12	10	11	9.35	4.66	9.63	4.66
9	12	10	10	9.89	14.70	10.21	15.03
10	10	11	10	−7.71	12.23	−6.77	12.03
11	10	11	11	−7.39	4.66	−6.49	4.66
12	10	11	12	−7.09	−2.30	−6.24	−2.13
13	10.292	11	12.707	−4.93	−6.86	−4.19	−6.67
14	11	11	13	−0.22	−8.61	0.44	−8.61
15	11.707	11	12.707	4.44	−6.74	5.17	−6.92
16	12	11	12	6.53	−2.19	7.36	−2.35
17	12	11	11	6.80	4.66	7.67	4.66
18	12	11	10	7.09	12.10	8.01	12.29

Woolnough, D.F., 1973. *A Fictitious Data Generator for Analytical Aerial Triangulation*, Technical Report 26, Department of Surveying Engineering, University of New Brunswick.

Appendix A

The Derivation for Rotation Elements

With the given projective center (X_C, Y_C, Z_C) and the direction of the optical axis (l, m, n), and assuming that the x-axis is parallel to the X-Y plane, the rotation matrix can be formulated.

(1) Let the z-axis of the image coordinate system coincide with the optical axis. The x-axis has the direction cosine (p, q, r). Because the x-axis is parallel to the X-Y plane of the object space,

$$r = 0. \tag{A1}$$

(2) Because the x-axis is perpendicular to the z-axis,

$$pl + qm + rn = 0. \tag{A2}$$

Therefore,

$$(p, q, r) = \begin{cases} \left(\dfrac{m}{\sqrt{l^2 + m^2}}, \dfrac{-l}{\sqrt{l^2 + m^2}}, 0\right) \\ \left(\dfrac{-m}{\sqrt{l^2 + m^2}}, \dfrac{l}{\sqrt{l^2 + m^2}}, 0\right) \end{cases} \tag{A3}$$

One should always take the positive sign for $\sqrt{l^2 + m^2}$ because it serves normalization.

(3) With a right-hand system, the direction cosine (u, v, w) of the y-axis can be expressed with the vector product,

$$(u, v, w) = (l, m, n) \times (p, q, r) \tag{A4}$$

$$\text{or} \quad = \begin{cases} \left(\dfrac{ln}{\sqrt{l^2 + m^2}}, \dfrac{mn}{\sqrt{l^2 + m^2}}, \dfrac{-l^2 - m^2}{\sqrt{l^2 + m^2}}\right) \\ \left(\dfrac{-ln}{\sqrt{l^2 + m^2}}, \dfrac{-mn}{\sqrt{l^2 + m^2}}, \dfrac{l^2 + m^2}{\sqrt{l^2 + m^2}}\right) \end{cases} \tag{A5}$$

The resulting rotation matrix is, then,

$$\mathbf{R} = \begin{pmatrix} \dfrac{m}{\sqrt{l^2 + m^2}} & \dfrac{-l}{\sqrt{l^2 + m^2}} & 0 \\ \dfrac{ln}{\sqrt{l^2 + m^2}} & \dfrac{mn}{\sqrt{l^2 + m^2}} & \dfrac{-(l^2 + m^2)}{\sqrt{l^2 + m^2}} \\ l & m & n \end{pmatrix},$$

$$\text{or} \quad \begin{pmatrix} \dfrac{-m}{\sqrt{l^2 + m^2}} & \dfrac{l}{\sqrt{l^2 + m^2}} & 0 \\ \dfrac{-ln}{\sqrt{l^2 + m^2}} & \dfrac{-mn}{\sqrt{l^2 + m^2}} & \dfrac{(l^2 + m^2)}{\sqrt{l^2 + m^2}} \\ l & m & n \end{pmatrix} \tag{A6a,b}$$